Fracture Mechanics of Concrete and Concrete Structures - Assessment, Durability, Monitoring and Retrofitting of Concrete Structures- B. H. Oh, et al. (eds)

Gas permeability of macro-cracked concrete: effect of temperature and water saturation

Wei Chen & Frédéric Skoczylas
Laboratoire de Mécanique de Lille (LML), Ecole Centrale de Lille, BP 48, F-59651 Villeneuve d'Ascq Cedex, France

ABSTRACT: This experimental work investigates the hydraulic behavior of a macro-cracked concrete, in order to improve the understanding of the coupled effects of temperature and water saturation. A concrete sample is macro-cracked using the Brazilian test technique. It is then submitted to dry or wet gas flow at different temperatures and confining pressures and its permeability is recorded. This first phase of the study clearly shows that confinement, which induces macro-crack closure, drives the first-order variation of permeability without any significant self-sealing of the crack, despite the wet gas injection. On another hand, injection of liquid water leads to a continuous decrease in flow rate. In a second phase, the permeability of intact, uncracked, material is measured under different moderate temperatures, which generates sample cooling or heating. This phase clearly demonstrates the importance of the sample initial saturation rate. Indeed, if the material is initially dry, temperature plays no role upon permeability, whereas it does if the material is initially partially water-saturated.

1 INTRODUCTION

This study is part of a large experimental program conducted by our laboratory upon the hydraulic behavior of concrete and upon the thermal conditions which affect this behavior. Numerous engineering problems require the knowledge of hydraulic behavior of cement-based materials under varying temperature. Such problems include thermal methods of oil recovery, geothermal reservoir engineering, storage of thermally active (mainly radioactive) wastes at low or great depth. In particular, as regards the design of safe confinement structures for nuclear power plants, the identification of gas flow mechanisms through porous, cracked, or pre-cracked areas is necessary to simulate accidental situations, so that the overall leakage should not exceed a safety limit. A special interest has to be given to cracked areas submitted to gas flow under different kinds of stresses and conditions of humidity and temperature. On real structures, contrasted gas permeability is also observed between summer and winter seasons: leakage rates are higher in summer. In first instance, the main difference is a higher temperature and a lower humidity level in summer. Some additional phenomena may also be accounted for: expansion and opening of cracks, local skin de-saturation leading to an increase in effective gas permeability, contraction of the concrete capillary pores during the colder winter period, etc. Therefore, our experimental investigations are carried out in order to investigate (1) the effect of hydrostatic loading, temperature and fluid water content upon gas permeability of a macro-cracked concrete, and (2) the effect of moderate temperature variations and saturation rate upon intact concrete gas permeability.

2 EXPERIMENTAL METHOD

2.1 *Material and sample preparation*

The concrete is composed of Type V cement (reference CEM V/A), sand (0-4mm), gravel (5-12mm) and an amount of water need-reducing additive. The mixture is prepared with a W/C ratio of 0.39. Large beams are made and kept for 28 days in lime-saturated water at a constant temperature of 20°C. Concrete samples are cylinders of 37 mm diameter and 60 mm height. They are cored from the beams after 28 days and rectified to obtain a proper planarity of their end surfaces. Reference dry state is taken after oven-heating at 60°C until constant mass. To obtain partially-saturated samples from an initial fully water-saturated state, samples are put in a climatic chamber which can control temperature and humidity, until mass stabilization. Concrete samples are macro-cracked along a diametral plane by the Brazilian test technique of traction-splitting (Figure 1). However, it is not possible to control their initial opening, see Figure 2. This leads to differences in the initial crack behavior vs. confining pressure: the

first crack closure obtained under increasing confining pressure is very different from one sample to another.

2.2 *Gas permeability measurement under isothermal conditions*

A steady state gas flow test apparatus (see Figure 3) is used to measure gas permeability at either ambient temperature or above (Loosveldt et al. 2002; Chen et al. 2009). The sample is placed inside a triaxial pressure cell and initially subjected to a hydrostatic stress, i.e. a confining, pressure P_c, while a constant gas pressure P_i is applied on one end and atmospheric pressure P_0 on the other. Confining pressure is held constant using a Gilson-type pump.

At ambient temperature, this test provides a *direct* measurement of the permeability by applying Darcy's law. A quasi-steady flow state method, based on an average gas volume flow rate Q_m measurement through the sample when decreasing slightly P_i by $\Delta P_i \ll P_i$, is performed at a mean gas pressure value $P_m=P_i-(\Delta P_i/2)$ (Skoczylas, 1996; Meziani & Skoczylas, 1999; Loosveldt et al., 2002). Permeability K along sample height L is given by Darcy's law as:

$$K = \frac{\mu Q_m}{A}\frac{2LP_m}{\left(P_m^2 - P_0^2\right)} \qquad (1)$$

where μ is gas viscosity. It is taken at a value of 2.2×10^{-5} Pa.s at 20°C for argon. P_i is set at 0.5MPa or at 1.0MPa and P_0 is atmospheric pressure.

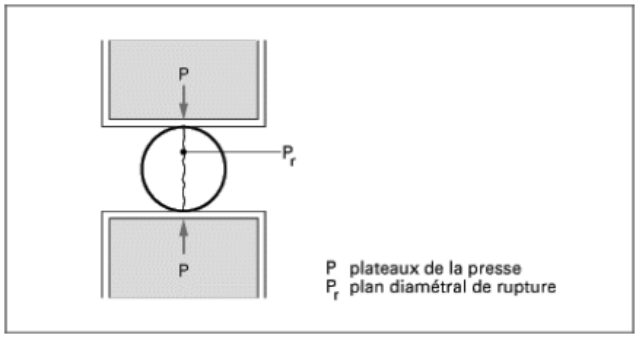

Figure 1. Sketch of the Brazilian splitting test, after (Davy et al. 2007).

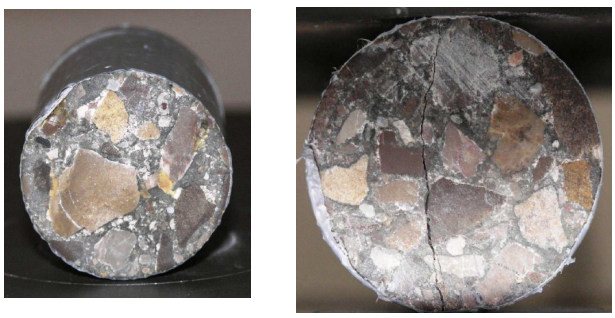

Figure 2. macro-cracked samples for gas permeability tests.

2.3 *Gas permeability measurement under non isothermal conditions*

Usually, the mean volume flow rate Q_m is measured at ambient temperature T_o. If the triaxial cell and the sample are at a different temperature T, the volume flow rate and the permeability calculation must be corrected; we must also take into account the viscosity variation in equation (1) as:

$$\mu(T) = \mu_{ref}\left(\frac{T}{T_0}\right)^{0.72} \qquad (2)$$

where T and T_0 are expressed in kelvin (ambient temperature is at 293K) and $\mu_{ref}=2.28\times10^{-5}$ Pa.s (R. Lide. 2001).

At constant pressure, for an ideal gas one can derive:

$$\frac{P}{\rho(T)} = \text{cste } T \text{ from where } \rho(T) = \left(\frac{T_0}{T}\right)\rho_0 \qquad (3)$$

and ρ_0 is $\rho(T_0)$.

If Q is the mass flow rate, it is constant in steady state, and the volume flow rate $Q_m(T)=Q/\rho(T)$. Therefore we have the following correction for Q_m:

$$Q_m(T) = \frac{T}{T_0}Q_m(T_0) \qquad (4)$$

Equations (1), (2) and (4) provide finally $K_X(T)$:

$$K_x(T) = \left(\frac{T}{T_0}\right)^{1.72} K_x(T_0) \qquad (5)$$

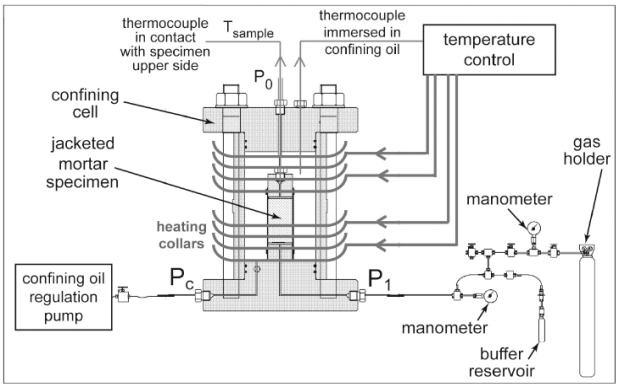

Figure 3. Experimental set-up used for continuous gas permeability tests under confinement and with temperature above ambient, from (Chen et al. 2009).

2.4 *Measurement devices for crack closure*

A LVDT device was especially designed to measure crack closure amplitude. To improve measurement accuracy, four LVDT sensors are used and placed in the sample median plane at 90° from one another (Fig. 4 and Fig. 5). If the sensors in opposition

measure respectively δ_1 and δ_2, the opening of the crack is given by:

$$e = \sqrt{\delta_1^2 + \delta_2^2}$$

where δ_1 is the displacement of diametrically opposed sensors 1 and 2. δ_2 is the displacement of diametrically opposed sensors 3 and 4.

2.5 *Test calibration*

This LVDT device must be carefully calibrated to evaluate the deformation of the assembly (mainly, the nylon support ring), the deformation of the Viton^{TM} sleeve, and the actual bulk deformation of the material. As a result, the crack opening/closure can be isolated, and will be presented hereafter.

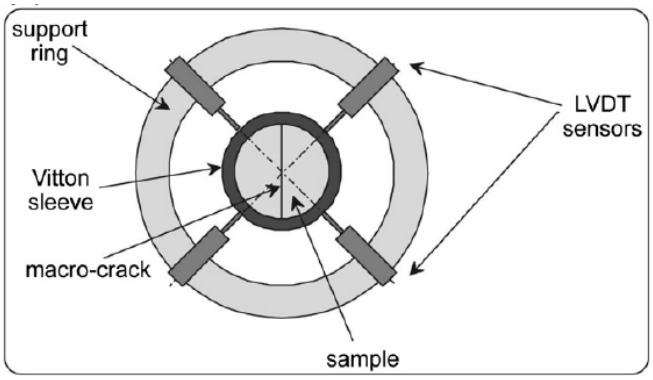

Figure 4. LVDT device, from (Davy et al. 2007).

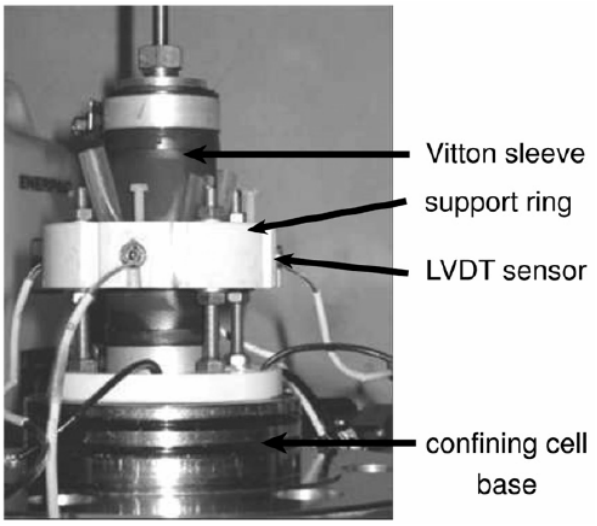

Figure 5. LVDT sensors and support ring, from (Davy et al. 2007).

2.6 *Experimental procedure*

During tests at ambient temperature, each macro-cracked sample is instrumented using the LVDT device in order to measure the crack displacement. The maximum level of confinement is 45MPa and the injection pressure for gas has been chosen in a range of 0.5 to 1.0 MPa. There distinct phases are considered:

1) During the first loading phase, confining pressure only is increased. Initial closure is unrepresentative of the macro-cracked concrete behavior, because the crack opening after initial splitting is not controlled. This phase is irreversible and has no real meaning for a structure because it is usually too large as compared to *in situ* cracking. The response of this "initial" crack is named "sample initial setting".

2) During subsequent loading phases, a reproducible crack behavior is observed. It is nonlinear elastic, and displays a bi-univocal relationship between confining pressure and crack amplitude, during loading and unloading. Crack amplitude in this phase is controlled by the sole confinement.

3) In this last phase, we inject the crack with wet and hot air (at 92% RH) for 48h to 5 days. This gas flow is carried out by a vacuum pump, which extracts air from the climatic chamber before flowing it through the crack. After humid gas flow is stopped, permeability is measured using the technique detailed in 2.3., with a *dry* gas flow.

Gas permeability is measured mainly during Phase (2) and Phase (3), and it is always performed using dry gas, under varied temperatures.

3 RESULTS

Tests described in Section 3.1, 3.2. and 3.4. are all at ambient temperature, whereas those described in Sections 3.3. and 3.5. are under temperature.

3.1 *Relationship between confining pressure and crack amplitude*

As mentioned above, the first phase of crack closure after the initial split has to be isolated from subsequent phases, which have less amplitude and are reproducible. First sample N°1 illustrates this assertion (Figure 6). We can see that the so-called “mechanical closure” occurs at ca. 20MPa confining pressure, above which the crack amplitude remains almost constant (vertical behaviour). It is assumed that its remaining small changes and "oscillations" are more related to sensor limits and calibration corrections, which are based on an average behaviour of the sensor device. Crack closure amplitude after Phase (1) is repeatable over the successive loading/unloading cycles and it is small, with a value of ca. 15 microns only.

Figure 7 compares the initial crack closure phase (1) for Samples N°1 and N°2. This shows a comparable behavior, yet with different total closure amplitudes. However, if we examine successive loadings (Figure 8), we can observe that after two to three loading-unloading cycles only, the initial difference has vanished: the crack behavior is virtually identical from one sample to the other. As a partial con-

clusion, after a few loading-unloading cycles, the mechanical behavior of two different samples is almost identical, although the initial crack aperture was different.

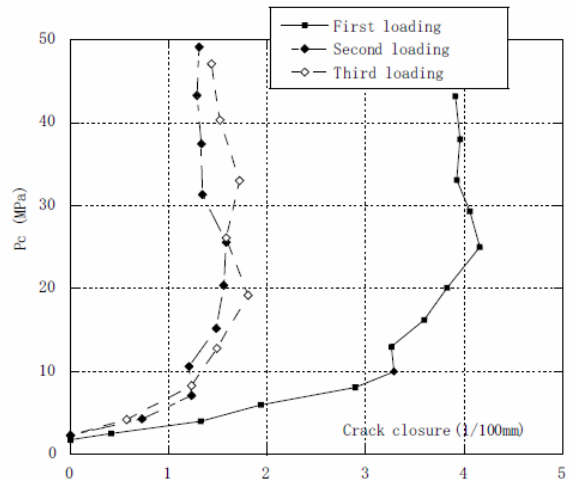

Figure 6. Three consecutive loading phases Pc vs. crack amplitude (or closure) for Sample N°1: initial confinement (Phase (1), represented on the right), and two subsequent loadings (Phase (2), represented on the left).

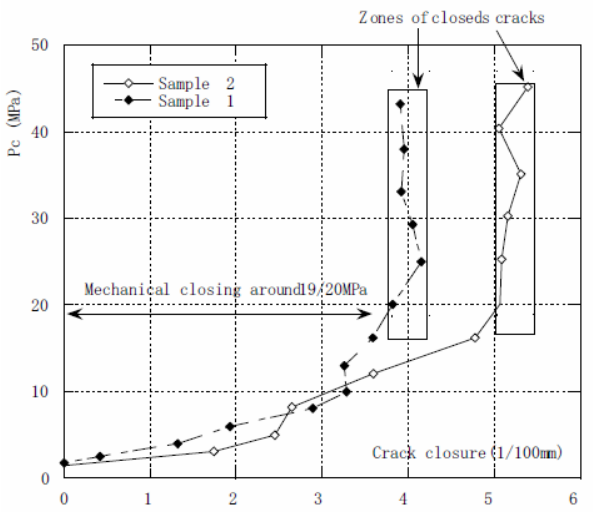

Figure 7. Comparison of initial closures for two different samples N°1 and N°2.

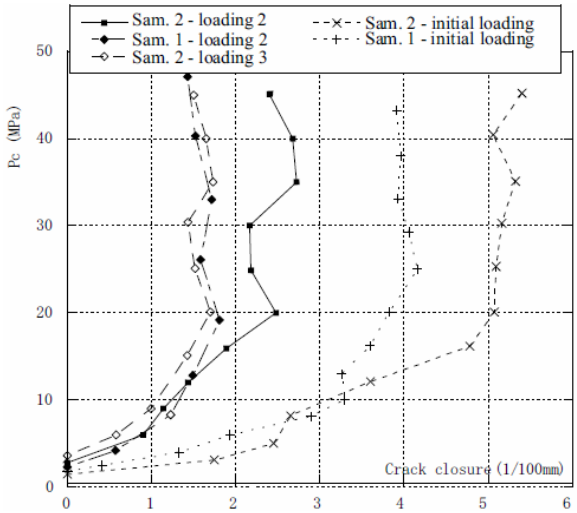

Figure 8. Comparison of crack closure for two samples – initial closure and reproducible.

3.2 *Relationship between confining pressure and gas permeability*

It is also necessary to put aside the initial closure phase in terms of gas permeability evolution. Indeed, in Figure 9, we can clearly observe that permeability variation is very sharp until the first mechanical closure occurred (around 20MPa) and this phase (1) is irreversible. In further cycles and whatever the injection pressure, gas permeability varies in a very narrow zone and is reversible. We can also notice that the first unloading cycle falls within this zone. Also, there is no significant effect of injection pressure P_i (taken equal to 1 or 0.5MPa) i.e. no visible Klinkenberg effect. Finally, even if the crack is mechanically closed, gas permeability varies very little around $10^{-15}m^2$, although it decreases continuously with confining pressure. It appears that, contrarily to mechanical closure, no hydraulic closure can ever be obtained.

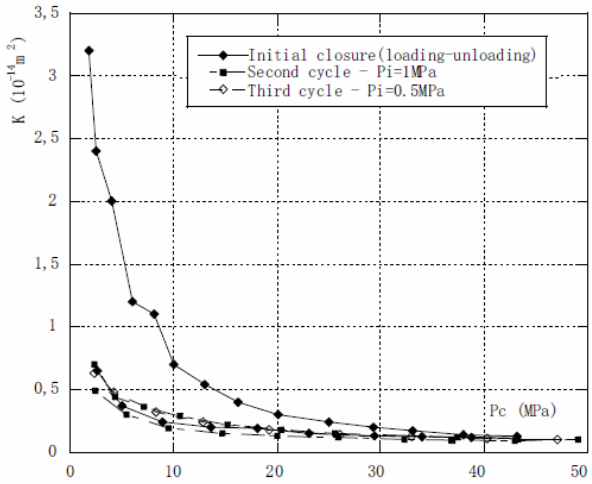

Figure 9. Sample N°1 – Gas permeability as a function of successive confining pressure increases and decreases. Gas and sample are at ambient temperature.

3.3 *Influence of humidity and low temperature variation*

In this part, the experiment consisted in flowing humid air (92% RH) at 24°C or at 50°C for at least 48h, then for periods of 5 consecutive days, through a non-confined crack. As rehydration may occur, the crack permeability is measured under increasing confinement. After humid air flow is stopped, the permeability test is performed by injecting dry argon gas into the heated triaxial cell, at either room temperature or at 50°C (identical to the humid air temperature). These phases can then be repeated.

Results of the first campaign (on Sample N°1) are not marked by a noticeable effect of successive humid air flow phases upon gas permeability (Figures 10-11), so that it appears that permeability still mainly depends upon confinement. The global trend is that of a slight decrease in permeability with accumulated cycles. On another hand, this slight de-

crease also depends upon injection pressure (0.5MPa to be compared to 1MPa, see Figs. 10 and 11), which might be due to the Klinkenberg effect, but it is so limited that it is hard to conclude at this point.

Sample N°2 is tested using similar cycles (Figure 12) at either ambient temperature, 35°C or 50°C and using 0.5 and 1 MPa gas injection pressures for permeability measurements. Sample N°2 evolution is almost identical to that of Sample N°1, indicating the predominance of confinement upon permeability variation. Again, there is no clear influence of sample temperature when humid air flows through the crack, all permeability vs. confining pressure behaviors are situated in a narrow zone.

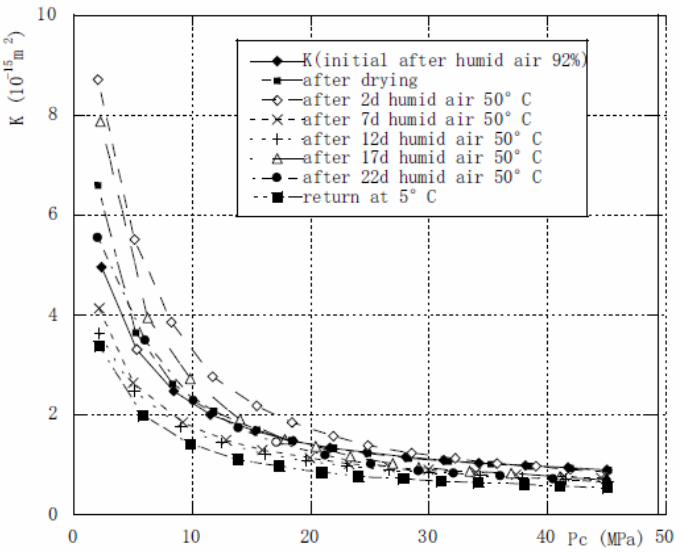

Figure 10. Evolution of gas permeability at 0.5MPa injection pressure, after several days humid air cycles (2 days, 7, 12, 17 or 22 days humid air injection) and at ambient temperature or at 50°C.

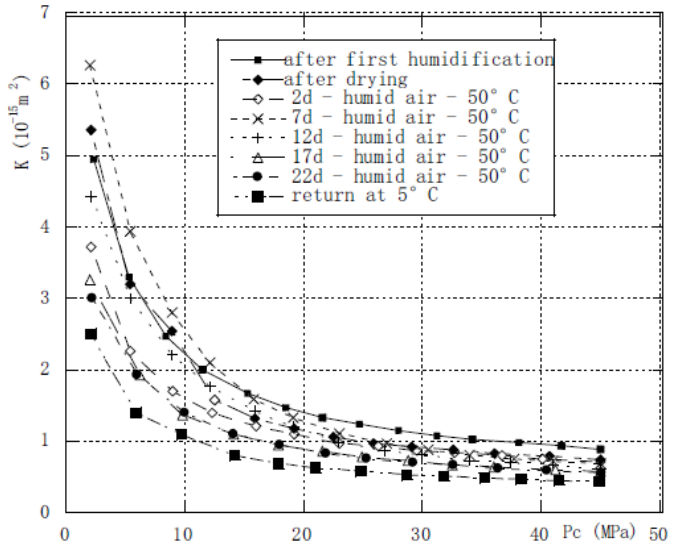

Figure 11. Evolution of permeability - at 1MPa injection pressure, after several days humid air cycles (2 days, 7, 12, 17 or 22 days humid air injection) and at ambient temperature or at 50°C.

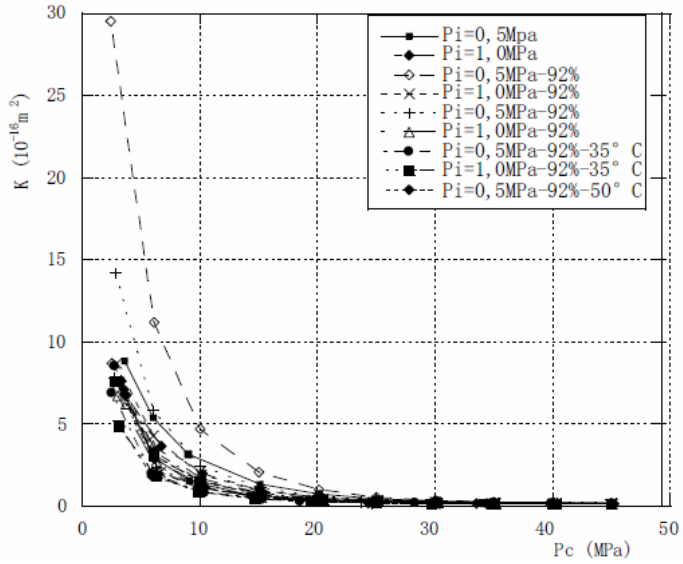

Figure 12. Evolution of permeability - at either 0,5MPa or1MPa injection pressure during humid air cycles, and with different temperatures.

3.4 *Effect of liquid water injection through macro-cracked concrete*

If humid gas does not induce significant changes in macro-crack permeability, what happens when water is injected through the macro-crack? Does self-sealing occur as in argillite (Davy et al. 2007)? In order to investigate this, a single preliminary test was conducted on Sample N°1, at 3 MPa confining pressure and using a gas injection of 0.5MPa. Results show a regular decrease in permeability and water flow (Figures 13 and 14). Moreover, one order of magnitude in water permeability is lost with time (from $9x10^{-17}m^2$ down to $10^{-17}m^2$ over 14 days), and water permeability is much lower than gas permeability (which has values of ca. 10^{-14}-$10^{-15}m^2$). The continued decrease in permeability (and flow) is related to macro-crack clogging in relation with cement re-hydration.

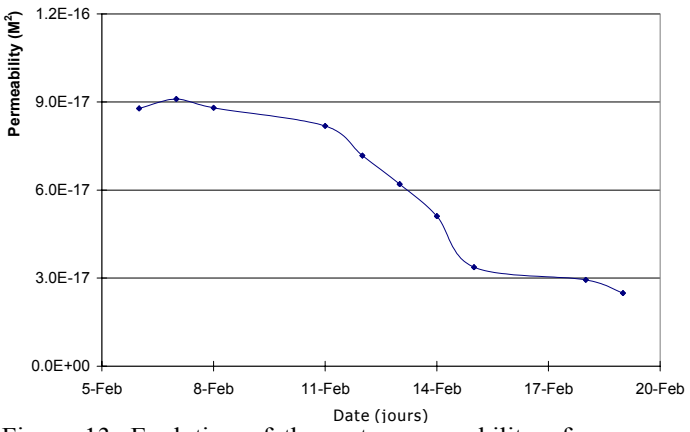

Figure 13. Evolution of the water permeability of a macro-cracked concrete sample.

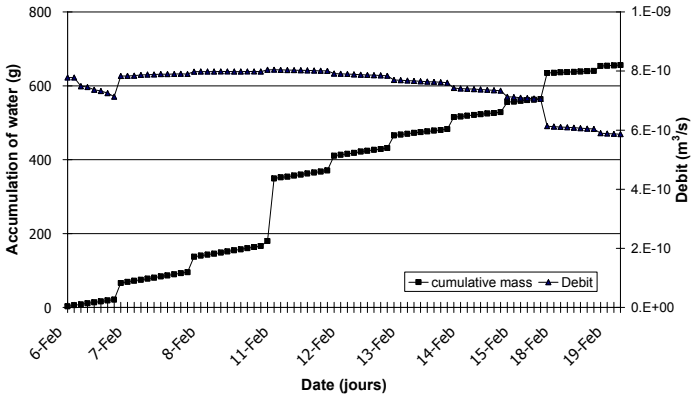

Figure 14. Water flow evolution in a macro-cracked concrete sample (in black, left vertical coordinates: water cumulative mass, in blue, right vertical coordinates: volume flow rate).

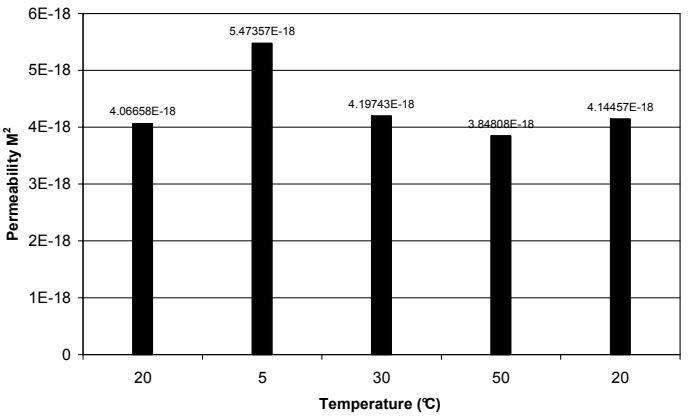

Figure 15. Permeability evolution for one single dry sample N°3 with temperature variations (20, 5, 30, 50 and 20°C successively).

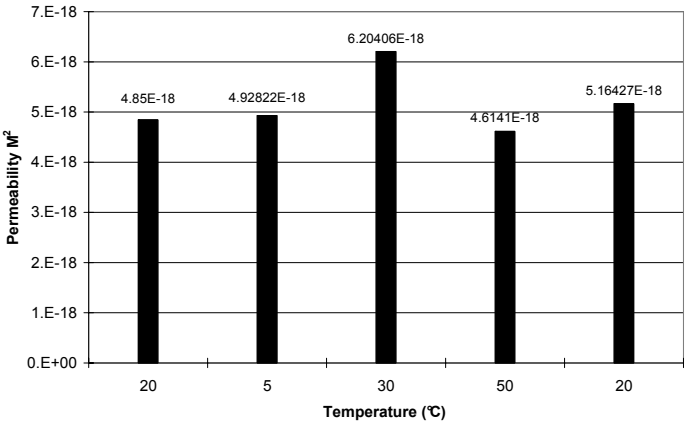

Figure 16. Permeability evolution for one single dry sample N°4 with temperature variations (20, 5, 30, 50 and 20°C successively), tested during 3 months.

3.5 *Effect of winter-summer cycling*

In this experiment, we have considered initially dry or partially-saturated concrete samples to assess the effect of water saturation upon dry gas permeability when temperature is varied within the range of European seasonal variations (i.e. between 5 and 50°C). We have adopted the following cycling method:

1. Initial gas permeability test at room temperature (20°C).
2. Gas permeability test at 5°C, by placing both triaxial cell and sample in a refrigerator chamber.
3. Gas permeability test at 30°C, then at 50°C or 40°C using the cell depicted in Figure 3.
4. Gas permeability test at 20°C, or again at 5°C

3.5.1 *Results for initially dry concrete*

Results for two initially dry samples N°3 and 4 (Figures 15 and 16) clearly show that gas permeability is reproducible and similar values are obtained whatever the temperature, and although they are 3 months apart from each other, for one same sample. It is to be emphasized that no significant influence of temperature occurs upon gas permeability when the material is initially dry. Another remarkable point is the magnitude of intact concrete permeability, as compared to macro-cracked material. It may be considered as intrinsic and, with values of ca. 4 to $5x10^{-18}m^2$, it is significantly lower than that obtained for macro-cracked sample (with values on the order of 10^{-14}-10^{-15} m^2), even when the macro-crack is mechanically closed. In addition, in terms of industrial relevance in the domain of nuclear power plant concrete structures, we can state that there is no seasonal difference in leakage rate when concrete is sound (i.e. un-cracked) and dry (which is not the case *in situ*).

3.5.2 *Results for initially partially saturated concrete*

Figures 17 and 18 present permeability results for two initially partially saturated samples N°5 and N°6. Initial partial saturation is obtained by placing both samples in a 60% RH atmosphere until constant mass, which leads to a water saturation level S_w of around 70%. This is considered as representative of *in situ* situations. Results are not ambiguous and saturation induces sensible effects upon gas permeability, with generally lower values when concrete is cooled rather than heated. If only little difference is noticed during retraction or expansion of an initially dry matrix (see 3.5.1.), it is no longer the case if pores are partially water-filled. Figure 17 shows that returning to 20°C provides sample N°5 with lower permeability than during the first measurement, while the return to 5°C for sample N°6 (Figure 18) induces a slightly higher permeability than that at the initial state. As our measurements do not change either the saturation or the micro-structure, we assume these differences to be due to a redistribution of the liquid phase in the capillary pores. Dilatometric contrasts between water and cement matrix induce redistribution of local pore water, which leads to variations in gas permeability (Chen et al. 2009).

More generally, the hot/cold cycles affect gas permeability measured at the same temperature. These early results clearly indicate that initial water saturation plays an important role upon concrete permeability when temperature varies, even moderately. Another clear trend is also that concrete is less permeable when cooled.

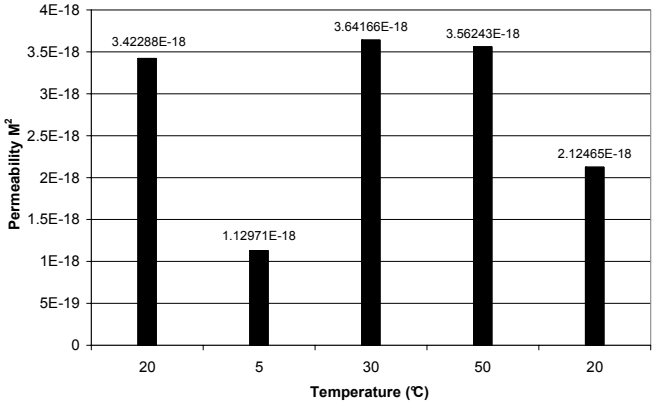

Figure 17. Temperature effect upon gas permeability for initially partially-saturated sample N°5 (20, 5, 30, 50 and 20°C successively).

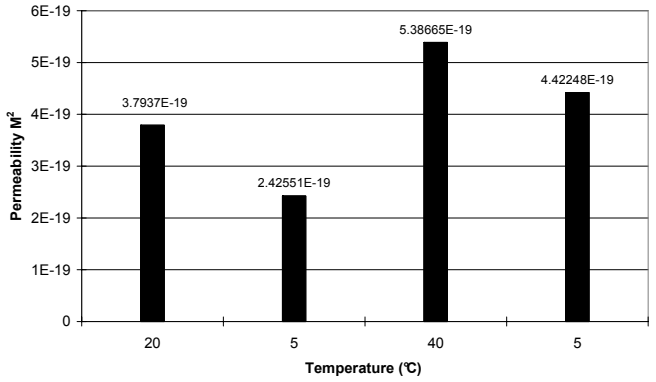

Figure 18. Temperature effect upon gas permeability for initially partially-saturated sample N°6 (20, 5, 40 and 5°C successively).

4 CONCLUSION

Permanent dry gas flow tests for macro-cracked concrete show that permeability K depends mainly upon crack closure, with values on the order of 10^{-14}–$10^{-17}m^2$. Crack closure itself being driven by confining pressure P_c, K also depends largely on P_c, during the initial loading/unloading phase as well as during the subsequent ones. There are, indeed, two successive steps: a first irreversible closure that is scarcely significant and non reproducible. It depends upon the initial crack opening, which is difficult to control. After this first loading step, the overall amplitudes of opening and closing are small and around 15-20 microns, associated to a nonlinear elastic relationship between crack amplitude and confining pressure P_c. In this second phase, gas permeability is well represented as a function of confinement only. Besieds, gas permeability depends very slightly upon gas injection pressure (0.5 or 1 MPa). Mechanical closure, whereby crack closure does not evolve any more, is obtained for all tests from around 18-20MPa. Nevertheless, after mechanical closure, an increase in confinement still leads to a continuous decrease in gas permeability. This means that there is a remaining intra-crack hydraulic path whatever the hydrostatic stress level. Injection of humid air through the crack shows very limited effect upon gas permeability, as compared to initial dry state. It appears that confining pressure solely drives gas permeability variation.

The injection of liquid water through macro-cracked concrete shows a steadily decreasing water flow rate over time, synonymous with lower water permeability. Our interpretation is that, in such situation, liquid water is able to induce macro-crack self-sealing, thanks to the rehydration of some anhydrous cement particles present at the crack lip surfaces.

Alternating summer and winter temperature variations shows the importance of initial water saturation rate. When concrete is initially dry, transition from hot to cold temperatures, and its reverse, induce no significant permeability variation. On another hand, pore water presence clearly changes gas permeability when temperature varies. In such case, gas permeability of colder material is consistently lower than that of heated material. As regards the industrial application of nuclear power plants, this may partly explain a leak rate slightly greater in summer than in winter, even in the absence of macro-crack. In addition, if water saturation gradients exist, for instance, in a thick confining structure wall, there will be structural permeability variations due to both lower saturation rates and cracking.

REFERENCES

Chen X.-T., Rougelot Th., Davy C.A.; Chen W., Agostini F., Skoczylas F., Bourbon X., 2009 Experimental evidence of a moisture clog effect in cement-based materials under temperature, Cement and Concrete Research, *in press*.

Davy C.A., Skoczylas F., Barnichon J.-D., Lebon P., 2007 Permeability of macro-cracked argillite under confinement: gas and water testing. Physics and Chemistry of the Earth 32:pp. 667-680.

Lide D. R. (Ed. in Chief). CRC Handbook of Chemistry and Physics. 82nd Ed.,CRC Press, Boca Raton, FL, 2001.

Loosveldt H., Lafhaj Z., Skoczylas F., 2002. Experimental study of gas and liquid permeability of a mortar. Cement and Concrete Research 32: pp.1357–1363.

Meziani H., Skoczylas F., 1999. An experimental study of the mechanical behaviour of a mortar and of its permeability under deviatoric loading. Materials and Structures 32 : pp.403–409.

Skoczylas F., 1996. Ecoulements et couplages fluide-squelette dans les milieux poreux. Etudes expérimentales et numériques. (in French) Mémoire d'Habilitation à Diriger des Recherches, Université des Sciences et Technologies de Lille, France.